MODELING AND SIMULATION OF 2D, ELECTROOSMOTIC FLOW (EOF) IN A SLIT CHANNEL WITH JOULE HEATING EFFECT

Barbaros CETIN , Dongqing LI
Vanderbilt University, Mechanical Engineering Department
VU Station B 351592, 2301 Vanderbilt Place, Nashville, TN, USA 37235-1592
Phone: +1 615-343-0473, Fax: +1 615-343-6687, e-mail: barbaros.cetin@vanderbilt.edu

ABSTRACT

In this study, the dynamic behavior of EOF and temperature field in a slit channel is simulated including the Joule heating effect. The flow field is copmposed of two parallel streams that have the different ionic concentrations. The channel is assumed to have finite length, and the thermal end effects are included in the model. The viscosity, thermal conductivity and dielectric constant of the fluid are taken as a function of temperature. Both constant and temperature dependent zeta potentials at the wall are considered.

Keywords: EDL, EOF, Joule heating.

1. INTRODUCTION

When a microchannel filled with an aqueous solution, there forms an Electrical Double Layer (EDL) field near the interface of the channel wall and the liquid. If an electric field is applied along the length of the channel, an electrical body force is exerted on the ions in the diffuse layer. In the diffuse layer of the EDL, the net charge density is not zero. The net transport of ions is the excess counterions. If the solid surface is negatively charged, the counterions are the positive ions. These excess counterions will move under the influence of the applied electrical field, pulling liquid with them and resulting in electroosmotic flow (EOF). The liquid movement is carried through to the rest of the liquid in the channel by viscous forces.

EOF is not very robust, as they depend sensitively on the physicochemical properties of the solution and channel walls. EOF depends on the walls' charge density, which varies with solution pH, ionic strength, and uncontrollably when solute molecules adsorb onto the walls. Besides its some adverse effects such as bubble formation introduction of pH or solute gradients associated with the electrochemical reactions occur in electrodes in order to maintain an electric field in solution, EOF is the most feasible way to control the fluid flow in microchannels due to the non-existence of moving parts and plug-like velocity profile. Moreover, channel size reduction and more understanding gained about this phenomenon in microchannels may diminish these adverse effects. In today's technology, EOF is the principle way of manipulating fluid flow and species transport in microchannels to make chemical and biological analysis, such as clinical diagnoses, DNA scanning, electrophoretic separations, cell manipulation, cell separation, cell patterning, and molecular detection (Li,2004).

Due to the presence of electrical potential gradient in EOF, the Joule heating effect may become important for high electrical potential gradients. This effect leads to temperature gradients in the transverse and longitudinal directions which reduces the separation efficiency due to the band spreading of the charged analytes, and which may cause denaturation of proteins or nucleic acids (Xuan, 2004). The use of polymer based materials in the production of lab-on-chip devices such as PDMS increases the significance of Joule heating because of their low thermal conductivity. Therefore, the control of the fluid temperature in microfluidic systems have become more crucial for the overall performance of the devices. However, these temperature gradients inside the channels may be used for cell manipulations.

The temperature effects due to Joule heating on capillary zone electrophoresis (Grushka et al, 1989, Gobie and Ivory, 1990, Bello and Righetti, 1992), and on EOF (Xuan et al, 2004, 2004, Erickson et al, 2004, Tang et al 2003, 2004, 2004, 2005, 2006, 2006) have been investigated extensively.

Xuan et al (2004, 2004) studied the effect of Joule heating and thermal end effects (i.e. finite length channel with reservoirs) EOF in a microcapillary with temperature dependent fluid properties. They compared their full model with the previous simplified models, and pointed out that their full model results were superior to the previous models.

Erickson et al (2004) examined the Joule heating and heat transfer in PDMS T-shaped microchannel with PDMS upper substrate and two types of bottom (PDMS and Glass) both numerically and experimentally. They found that the PDMS/Glass channel maintained a much more uniform and lower buffer temperature than the PDMS/PDMS

Nomenclature

C	molar concentration (mole/l)
Cp	specific heat
$\vec{E}$	applied electric field
h_{conv}	convective heat transfer coefficient
k	thermal conductivity
L	channel length
p	hydrodynamic pressure
H	channel heigth
T	time
T	temperature
T_∞	Ambient temperature
$\vec{v}$	velocity field

Greek Symbols

σ	electric conductivity
ε	dielectric constant
ε_0	permittivity of the vacuum
λ	molar conductivity
μ	dynamic viscosity
φ	external potential field
ρ	mass density
ζ	zeta potential

channel due to the higher conductivity of the glass than PDMS. They also concluded that despite of the temperature dependence of the viscosity and electrical conductivity of the buffer the velocity field was undistorted because of the counter-balancing effects of the decreased viscosity and decreased potential field gradient in the hotter sections of the channel.

Tang et al studied the effect of Joule heating on EOF and mass species transport inside microtubes (2003, 2004, 2005, 2006), slit microchannels (2004) and rectangular microchannels (2006). They considered for electrokinetic mass transport both the continuous sample injection (2003, 2004, 2005, 2006), and finite length plug sample injection (2005, 2006, 2006). They found that the joule heating may result in significantly different EOF and mass species transport characteristics.

In this study, dynamic behavior of EOF and temperature field is analyzed for slit channel including the Joule heating effect with two parallel streams that have the different ionic concentrations by using commercial FEM based code FEMLAB®. The viscosity, thermal conductivity and dielectric constant of the fluid are taken as a function of temperature which leads to coupled temperature field, flow field, electrical double layer field and electrical potential field. The channel is assumed to have finite length, and the thermal end effects are included in the model. The zeta potential is considered both constant, and function of temperature.

2. ANALYSIS

2.1. Governing Equation

Fig 1 shows the geometry modeled in this work. This 2D model will be extended to 3D to simulate the microchannel with two end reservoirs, therefore the end temperatures are assumed to be equal to ambient temperature which will be the case in 3D modeling. Different from the conventional pressure driven flows, the driving force is the electrical body force in EOF. Therefore, the Navier-Stokes equation for laminar, incompressible flow can be written as,

$$\nabla \cdot \vec{\mathrm{v}} = 0 , \tag{1}$$

$$\rho\left[\frac{\partial \vec{\mathrm{v}}}{\partial t} + (\vec{\mathrm{v}} \cdot \nabla)\vec{\mathrm{v}}\right] = -\nabla p + \nabla \cdot \left[\mu(T)\nabla \vec{\mathrm{v}}\right] + \rho_e E , \tag{2}$$

where is the velocity vector, t is the time, ρ is the density of the liquid, p is the hydrodynamic pressure, $\mu(T)$ is the temperature dependent viscosity, T is the absolute temperature, ρe is the electric charge density, and E is the applied electric field. The temperature dependence of viscosity for liquids is significant; therefore, viscosity is taken as function of temperature to capture the velocity field distortions due to temperature gradients.

The electric field E is calculated from the externally applied electric potential φ by

$$\vec{E} = -\nabla \varphi . \tag{3}$$

Since the channel wall is non-conducting, the conservation of electric current equation yields

$$\nabla \cdot \left[\sigma(T)\nabla \varphi\right] = 0 , \tag{4}$$

where $\sigma(T) = \lambda(T)C$ is the temperature dependent electric conductivity where C is the molar concentration and is the molar conductivity of the solution. The molar concentration is function of bulk ionic concentration; therefore, it can be written as a function of molarity as

$$C = 1000M , \tag{5}$$

where M is the molarity of the solution.

The temperature field can be determined via energy equation which can be written in the presence of EOF as,

$$\rho C_p\left(\frac{\partial T}{\partial t} + \vec{v} \cdot \nabla T\right) = \nabla \cdot \left[k(T)\nabla T\right] + \sigma(T)\vec{E}.\vec{E} , \tag{6}$$

where C_p is the specific heat of the liquid and is assumed to be constant, $k(T)$ is the temperature

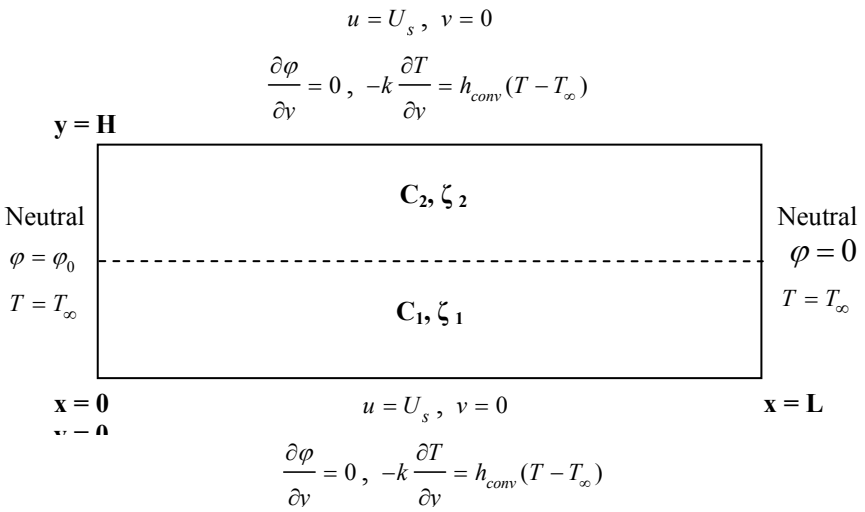

Fig 1 Solution domain and the boundary conditions

dependent thermal conductivity of the fluid. The last term in the energy equation stands for the Joule heating effect. The viscous dissipation term in the energy equation is neglected, since it is very small compared to the Joule heating due to the very low velocity inside the microchannel.

The driving mechanism for EOF is the electrical body force applied to the excess ions inside the electrical double layer (EDL); so the ion distribution inside the EDL is important for the analysis. Since the EDL thickness is very thin compared to the channel height, neglecting the EDL thickness (i.e. neglecting the electrical body force term in momentum equation) and introducing a slip velocity at the boundary is a common method to simulate the EOF which avoids the solution of the EDL field (Xuan et al, 2004). The same approach is used in this study, and slip velocity is imposed to the boundary condition of the Navier-Stakes equation which is defined as,

$$U_s = -\frac{\varepsilon(T)\varepsilon_0\zeta(T)}{\mu(T)}E_x, \qquad (7)$$

where $\varepsilon(T)$ is the temperature dependent dielectric constant, ε_o is the dielectric constant of the vacuum, and $\zeta(T)$ is zeta potential -the electric charge density formed by the charge at the capillary internal wall. E_x is the applied electric field strength in the x-direction.

Venditti et al (2006) mentioned the temperature dependence of ζ, and concluded that neglecting its dependence to T can result in the underestimation of the slip velocity in microfluidic applications. They also gave some experimental data for commonly-used buffers in both PDMS:Glass and PDMS:PDMS microchannels. Their experimental data showed that temperature dependence on temperature for PDMS:PDMS channels are negligible, and significant dependence on temperature for PDMS:Glass channels. In this study zeta potential assumed both constant and function of temperature, and the data of Venditti et al (2006) is used.

2.2. Boundary Conditions

For conducting media equation, Eq (4), boundary conditions specified as follows,

$\varphi = 300$ V at $x = 0$, (8-a)

$\varphi = 0$ at $x = L$, (8-b)

$\frac{\partial \varphi}{\partial y} = 0$ at $y = 0$ and $y = H$ (insulated). (8-c)

For the continuity and momentum equations, the neutral boundary condition option of the FEMLAB is used at the inlet and the exit of the channel, which is

$\left[pI + \mu(\nabla\vec{v} + (\nabla\vec{v})^T)\right]\cdot\hat{n} = 0$ at $x = 0$ and L, (9-a)

and the slip velocity, Eq (7) is used for the x-component, and zero for y-component of the velocity at the walls,

$u = U_s$ and $v = 0$ at $y = 0$ and $y = H$. (9-b)

For energy equations, the boundary conditions are defined as,

$T = T_\infty$ at $x = 0$ and $x = L$, (10-a)

$-k\frac{\partial T}{\partial y} = h_{conv}(T - T_\infty)$ at $y = 0$ and $y = H$, (10-b)

where h_{conv} is the convective heat transfer coefficient, and taken as 10 W/m^{2}K in this study, which is a reasonable value for a natural convection. The solution domain and the boundary conditions are summarized in Fig 1.

In the analysis, the transient term in the momentum equation is omitted, since the time to reach the steady state for velocity profile is in the order of microseconds (Li,2004). Therefore, only the transient term in the energy equation is considered. The initial condition for the energy equation is given as,

$$T(x, y) = T_\infty \text{ at } t = 0 . \quad (11)$$

2.3. Numerical Solution

The coupled equations, Eqs (1), (2), (4) and (6) should be solved together with the boundary conditions, Eqs (8)-(10), and the initial condition Eq (11) simultaneously to determine the flow field and the temperature field. The commercial code based on Finite Element Method, FEMLAB® is used to solve the equations. The neutral boundary condition for Navier-Stokes equation, and continuity boundary condition for energy and electrical potential equation (which equates the fluxes at the two sides of the boundary) are used for the artificial interface between the two streams.

Since the domain boundaries are regular, rectangular elements are used in the solution. A non-uniform grid is generated with grid refinement in the channel inlet and outlet as well as the region near the channel wall and the interior boundary between the parallel streams. 20x30 grids are used in the solution.

To solve the system, a guessed solution is needed to start the solution procedure. The slip velocity value at the initial temperature and uniform electric field is given as the initial value for the x-component of the velocity everywhere in the domain, and zero is assigned for the y-component of the velocity. The time for simulation is chosen as 50 s which is reasonable time to analyze the transient behavior. To run the simulation till it reaches the steady state is somehow unrealistic, since our thermal boundary conditions for the inlet and the exit *(T=T∞)* are reasonable for small t. Although the heat capacities of the reservoirs are large, they are finite in reality. So, for long time our inlet and exit boundary conditions would distort.

3. RESULTS and DISCUSSIONS

Electric, velocity and temperature field are determined by solving coupled electrical potential, Navier-Stokes and energy equation. The equations are solved by FEMLAB®. The viscosity, thermal and electrical conductivity of the fluid are taken as function of temperature. The interface between the two streams assumed to be impermeable for the ions. Therefore, the diffusion equation for ions is not solved, and the ionic concentration of the two streams is assumed to be constant along the channel which is not realistic. The results are examined in the presence of this simplification.

Since the ionic concentration of the streams is assumed to be constant, the zeta potential at the walls become only function of temperature. Two cases are considered:

(i) $C_1 = 10\ mM$, $\zeta_1 = -50\ mV$ and
$C_2 = 0.001\ mM$, $\zeta_2 = -250\ mV$

(ii) $C_1 = 10\ mM$, $\zeta_1 = -0.48T - 43.8\ mV$ and
$C_2 = 0.1\ mM$, $\zeta_2 = -0.06T - 107.4\ mV$

where T is in ^oC.

In case (i), the zeta potentials are assumed to be constant, since there is no experimental data available for C = 0.001 mM, and in the case (ii) the data of Venditti et al (2006) for PDMS:Glass channels is used. Basically, case (i) is to see the effect of large concentration difference, and case (ii) is to see the effect of temperature dependent zeta potential.

Constants	
Permittivity of vacuum	$\varepsilon_0 = 8.854\times 10^{-12}$ C^2/N m^2
Density	$\rho = 1000\ kg/m^3$
Ambient temperature	$T_\infty = 298$ K
Heat capacity	$C_p = 4180$ J/kgK
Height*	$H = 100\ \mu m$
Length*	$L = 4\ cm$
Applied electric field*	$E = 7.5\ kV/m$
Convective heat transfer coefficient*	$h_{conv} = 10\ W/m^2K$
Variables	
Dynamic viscosity	$\mu = 2.761\exp(1713/T)$ kg/ms
Thermal conductivity(W/mK)	$k = 0.61 + 0.0012(T - T_\infty)$
Molar conductivity($m^2 S/mole$)	$\lambda = 12.64\left[1 + 0.025(T - T_\infty)\right]$
Relative dielectric const.	$\varepsilon = 305.7\exp(-T/219)$

(*) unless otherwise stated

Table1 Summary of the input parameters

Table 1 summarizes input parameters used in the analysis. Most of the input parameters are taken same as in the study of Xuan et al (2004).

Fig 2 shows the transient development of the centerline temperature inside the channel for both cases. The temperature gradients are mainly at the inlet and the exit section. Since the ionic concentration is higher for the upper stream in case (ii) than the case (i), its electrical conductivity is

higher which leads to a higher Joule heating and higher temperature values. The length of the entrance region increases in time due to the advection of the cold solution in the inlet to the outlet. The effect is significant for case (i) because of the higher slip velocities due to the higher zeta potential in magnitude.

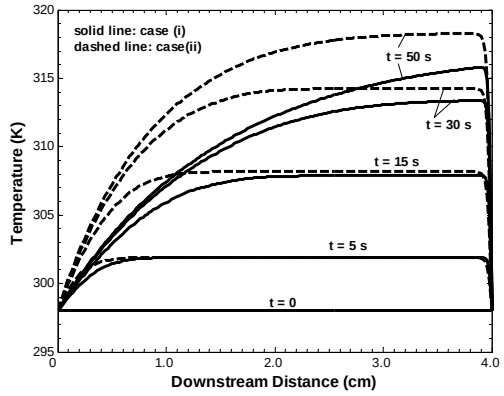

Fig 2 Transient development of the centerline temperature.

Fig 3 shows EOF velocity profile at different stream-wise locations for both cases. The velocity profiles are distorted from the uniform velocity profile (which is the case for uniform stream) due to the different slip velocities at the wall. The lower stream has the higher concentration and lower zeta potential, so the slip velocity at the lower wall is smaller than the one at the upper wall. The distortion from the uniform velocity profile is more significant for case (i) because of the larger difference between the concentrations of the two streams.

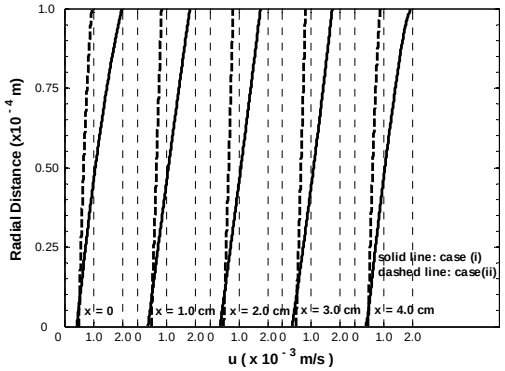

Fig 3 Electroosmotic velocity field after 50 s.

Since there is a velocity gradient along the channel, a pressure difference is induced along the channel. Fig 4 shows transient development of the induced pressure field. The pressure increases at the inlet, experiences a max; and then decreases, experiences a min and increases again (even it is not clear from the figure because of the scale). As the slip velocity and the average velocity increases in time, the induced pressure curve shifts to the up.

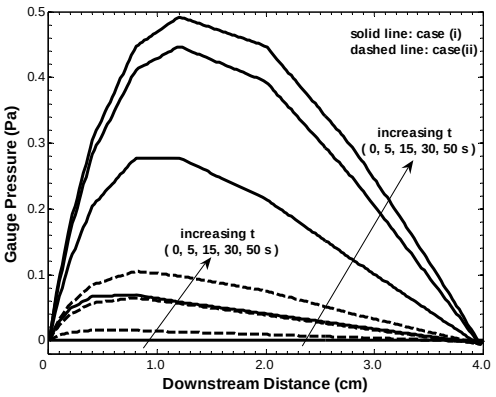

Fig 4 Induced pressure field after 50 s.

Fig 5 and Fig 6 shows the temperature profiles in transverse direction at different axial location after 50 s for two cases. The temperature axis is characterized by the temperature difference between the flow field and the upper wall (corresponding wall temperatures are given in the figure). At the inlet and outlet the temperature profiles are uniform and equal to the ambient temperature as a boundary conditions. By the presence of two streams, the temperature profile is no more symmetric about the centerline, and temperature gradient exists at the centerline unlike the uniform stream case. Unfortunately, the temperature change is very small due to the low Biot number (depend on the characteristic dimension at r-direction) of the system. Actually in practice, the temperature profile can be assumed to be uniform in r-direction.

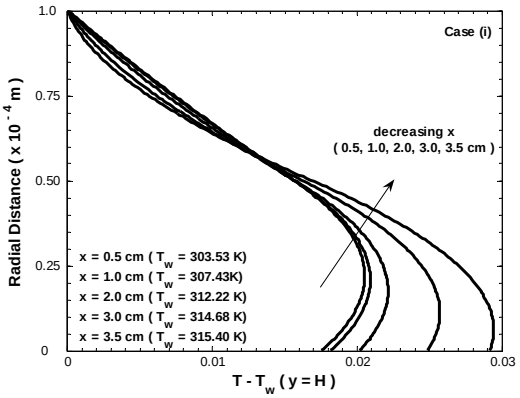

Fig 5 Temperature profiles in transverse direction at different axial locations after 50 s

The nose of the temperature profile shifts to the lower wall, since the lower stream has the higher thermal conductivity, and higher Joule heating. Moreover, the lower stream has the lower convection due to the decreases velocities compared to the upper stream. The behavior of the

temperature profiles is same for both cases, but the gradient at the centerline is lower for case (ii) due to the lower concentration difference between the two streams.

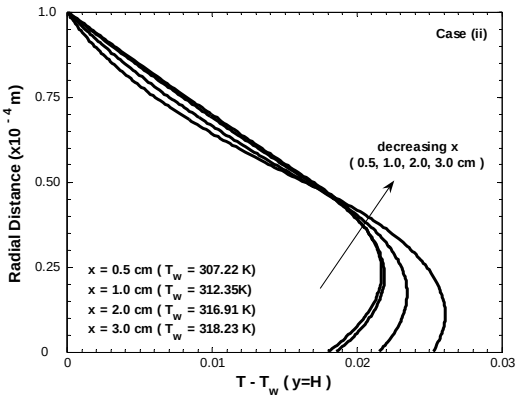

Fig 6 Temperature profiles in transverse direction at different axial locations after 50 s

Fig 8 shows the temperature profiles in transverse direction for different parameters at *x = 2 cm* after 50 s. In this graph, the effect of convective heat transfer coefficient, channel height and the strength of the electric field can be seen. For the case with 100 W/m^{2}K convective heat transfer coefficient; the gradient is small, and the temperature is close to the ambient temperature because the heat generated by the Joule heating is dissipated through the convective heat transfer from the walls (i.e. increased Biot number). For the case with higher electrical field strength, the gradient is higher due to the higher resistive heating inside the channel. Moreover the temperature is also high inside the channel *(Tw = 367.11 K)* which can cause the breakdown of the system. Increase of the channel height has the most significant effect on the temperature gradient inside the channel. The gradient increases for the case H = 300 μm, because of the increased Joule heating due to the increased volume of the channel. Increase in the channel height will also increase the power input to the system to create the same electrical potential difference along the channel.

4. CONCLUSIONS

In this study, the dynamic behavior of EOF and temperature field in a slit channel is simulated including the Joule heating effect with two parallel streams that have the different ionic concentrations. The viscosity, thermal conductivity and dielectric constant of the fluid are taken as a function of temperature. The channel is assumed to have finite length, and the thermal end effects are included in the model. The zeta potential is considered both constant and function of temperature.

The two parallel streams with different

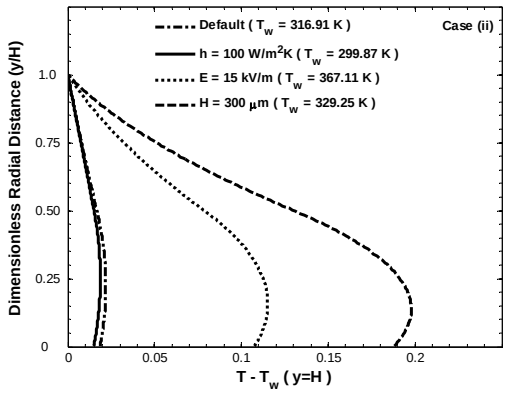

Fig 8 Temperature profiles in transverse direction for different parameters at *x = 2 cm*

concentrations are proposed to create a temperature gradient inside the channel -especially at the center- for the possible use of the extended 3D model of this model in cell manipulations. The effects of the different input parameters on the temperature profile across the channel are also discussed. Asymmetric temperature profile is obtained across the channel, but unfortunately, the temperature change are found not to be high enough to manipulate the cells.

The important assumption in this study is the constant ionic concentration of the two parallel streams which is not realistic. In reality the two streams would diffuse into each other, and the concentration would like to be uniform at the downstream which will lead to a symmetric (in r-direction) temperature profile at the far downstream even if there was an unsymmetric temperature at the upstream. However, even the presence of neglected diffusion, the achieved temperature gradients across the channel are found to be insufficient to manipulate cells.

REFERENCES

M. Bello, P. G. Righetti, Unsteady heat transfer in capillary zone electrophoresis: I. A mathematical model, *Journal of Chromatography*, 606, 1992, 95-102.
II. Computer Simulation, *Journal of Chromatography*, 606, 1992, 103-111.

D. Erickson, D. Sinton and D. Li, Joule heating and heat transfer in poly(dimethylsiloxane) microfluidic systems, *Lab Chip*, 2003, 3, 2003, 141-149.

W, A, Gobie, C. F, Ivory, Thermal model of capillary electrophoresis and a method for counteracting thermal band broadening, *Journal of Chromatography*, 516, 1990, 191-210.

E. Grushka, R. M. McCormick, J. J. Kirkland, Effect of temperature gradient on the efficiency of

capillary zone electrophoresis separations, Anal. Chem., 61, 1989, 241-246.

D. Li, Electrokinetics in Microfluidics, Elsevier Academic Press, 2004.

G. Y. Tang, C. Yang, C. J. Chai, H. Q. Gong, Modeling of electroosmotic Flow and Capillary electrophoresis with Joule heating effect: The Nernst-Planck Equation vs Boltzmann Distribution, *Langmuir*, 19, 2003, 10975-10984.

G. Y. Tang, C. Yang, C. J. Chai, H. Q. Gong, Joule heating effect on electroosmotic flow and mass species transport in a microcapillary, *International Journal of Heat and Mass Transfer*, 47, 2004, 215-227.

G. Y. Tang, C. Yang, C. J. Chai, H. Q. Gong, Numerical analysis of the thermal effects on electroosmotic flow and electrokinetic mass transport in microchannels, *Analytica Chimica Acta*, 507, 2004, 27-37.

G. Y. Tang, C. Yang, H. Q. Gong, C. J. Chai, Y.C. Lam, On electrokinetic mass transport in a microchannel with joule heating effects, *Journal of Heat Transfer*, 127, 2005, 660-663.

G. Y. Tang, C. Yang, H. Q. Gong, C. J. Chai, Y.C. Lam, Numerical simulation of Joule heating effect on sample band transport in capillary electrophoresis, *Analytica Chimica Acta*, 561, 2006, 138-149.

G. Y. Tang, D. Yan, C. Yang, H. Q. Gong, C. J. Chai, Y.C. Lam, Assessment of joule heating and its effects on electroosmotic flow and electrophoretic transport of solutes in microfluidic channels, *Electrophiresis*, 27, 2006, 628-639.

R. Venditti, X. Xuan, D. Li, Experimental characeriztaion of the temperature dependence of zeta potential and its effect on electroosmotic flow velocity in microchannels, *Microfluidics and Nanofluidics*, 2, 2006, 493-499.
.

X. Xuan, D.Sinton, D. Li, Electroosmotic flow with joule heating effects, *Lab Chip*, 4, 2004, 230-236.

X. Xuan, D.Sinton, D. Li, Thermal end effects on electroosmotic flow in a capillary, *International Journal of Heat and Mass Transfer*, 47, 2004, 3145-3157.